

---

# DarrenNet: Fully Convolutional Network for Semantic Segmentation

---

**Brandon Szeto** \*

Jacobs School of Engineering  
University of California, San Diego  
San Diego, CA 92122  
bszeto@ucsd.edu

**Darren Yu** †

Jacobs School of Engineering  
University of California, San Diego  
San Diego, CA 92122  
dmyu@ucsd.edu

**Nathaniel Thomas** ‡

Jacobs School of Engineering  
University of California, San Diego  
San Diego, CA 92122  
nathomas@ucsd.edu

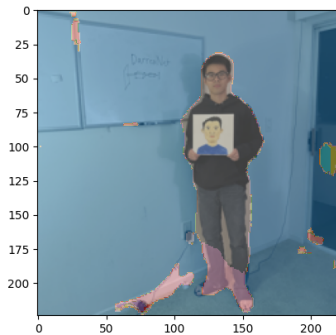


Figure 1: DarrenNet computing inference on Darren

## Abstract

This abstract provides a succinct overview of our work focused on semantic segmentation using the PASCAL VOC-2007 dataset. Our approach involves leveraging a novel deep learning architecture tailored for semantic segmentation tasks. We meticulously preprocess the dataset, addressing challenges such as class imbalance and data augmentation to enhance model generalization. Through experimentation, we explore hyperparameter tuning strategies to optimize performance. Our results showcase a notable improvement in both percent correct and Mean Intersection over Union (IoU) metrics, underscoring the efficacy of our methodology. Additionally, we uncover intriguing insights into the model’s behavior, shedding light on its strengths and potential areas for refinement. This work showcases a framework for accurate and nuanced semantic segmentation.

---

\*160 lbs

†130 lbs

‡200 lbs

## Introduction

Semantic segmentation is the task of assigning each pixel in an image a specified label. A single image can be partitioned into multiple meaningful segments corresponding to a given object or region of interest. Labels are assigned to individual pixels, marking boundaries and shapes. Altogether, this task has many applications in computer vision including but not limited to autonomous driving, video surveillance, and object recognition.

In recent years, convolutional neural networks (CNNs) have proven to be an effective approach to semantic segmentation. Such models learn hierarchical features by capturing information using convolutional blocks. Convolutions and related techniques such as weight initialization, batch normalization, and pooling help avoid the flat, dense layers of a traditional fully connected neural network allowing for less computation and improved feature maps.

### Xavier Weight Initialization

In our architecture, we use Xavier weight initialization. In Uniform Xavier Initialization, a layer's weights are chosen from a random uniform distribution bounded between

$$\pm \frac{\sqrt{6}}{\sqrt{n_i + n_{i+1}}} \quad (1)$$

where  $n_i$  is the number of incoming network connections and  $n_{i+1}$  is the number of outgoing network connections.

In Normal Xavier Initialization, a layer's weights are chosen from a normal distribution with

$$\sigma = \frac{\sqrt{2}}{\sqrt{n_i + n_{i+1}}} \quad (2)$$

where  $n_i$  is the number of incoming network connections and  $n_{i+1}$  is the number of outgoing network connections.

The Xavier initialization was created in response to the problem of vanishing and exploding gradients in deep neural networks in the context of symmetric nonlinearities (sigmoid, tanh). The intuition is that the weights should not be initialized randomly, but rather proportional to the size of two connected layers. As a result, the variance of activations and gradients would be maintained through the layers of a deep network.

### Kaiming Weight Initialization

With the rise of ReLU, the nonlinearity can no longer be assumed to be symmetric. As such, the assumptions made by the Xavier Weight Initialization fall apart. In 2015, He et. al demonstrated that a ReLU layer typically has a standard deviation close to

$$\sqrt{\frac{n_i}{2}} \quad (3)$$

where  $n_i$  is the number of incoming network connections. As such, weights initially chosen from a normal distribution should be weighted by  $\sqrt{\frac{n_i}{2}}$ , with bias tensors initialized to zero.

### Batch Normalization

During the training of a neural network, at each layer, inputs (activations) change as the parameters of the previous layers get updated. Batch normalization normalizes the activations of each layer by subtracting the mean and dividing by the standard deviation of the activations within a mini-batch. We implement batch normalization using PyTorch's nn module implementation. For example, we define a layer used for batch normalization as

```
self.bnd1 = nn.BatchNorm2d(32)
```

This ensures that the inputs to each layer have a consistent distribution, which helps in stabilizing the training process.

### Pixel Accuracy

Pixel accuracy is a straightforward evaluation metric commonly used in image classification tasks to measure the percentage of correctly classified pixels in an image. It provides a simple measure of overall accuracy without considering class imbalance.

Pixel accuracy is calculated as:

$$\text{Pixel Accuracy} = \frac{\text{Number of Correctly Classified Pixels}}{\text{Total Number of Pixels}} \quad (4)$$

Where:

- **Number of Correctly Classified Pixels:** The count of pixels for which the predicted class matches the ground truth class.
- **Total Number of Pixels:** The total count of pixels in the image.

While pixel accuracy provides a quick measure of overall performance, it may not be the most informative metric for tasks with class imbalance or when individual classes are of interest.

### Intersection over Union (IoU)

Intersection over Union (IoU), also known as the Jaccard index, is a popular evaluation metric in semantic segmentation tasks. It measures the overlap between the predicted segmentation mask and the ground truth mask for each class. IoU provides a more nuanced understanding of model performance by considering both true positives and false positives.

For a given class  $c$ , IoU is calculated as:

$$IoU_c = \frac{\text{Area of Intersection between predicted and ground truth mask for class } c}{\text{Area of Union between predicted and ground truth mask for class } c} \quad (5)$$

The overall IoU for all classes is often computed as the mean or weighted mean of individual class IoU scores:

$$IoU = \frac{1}{N} \sum_{c=1}^N IoU_c \quad (6)$$

Where:

- $N$  is the total number of classes.
- $IoU_c$  is the IoU score for class  $c$ .

IoU ranges from 0 to 1, with higher values indicating better segmentation accuracy. A value of 1 indicates perfect overlap between the predicted and ground truth masks, while a value of 0 indicates no overlap.

IoU is particularly useful for tasks where precise localization and segmentation accuracy are essential, such as medical image analysis, object detection, and scene understanding. It provides insights into how well the model captures the spatial extent of different classes within the image.

## Related Works

### U-Net

U-Net Ronneberger et al. [2015] has proven to be highly effective for biomedical image segmentation tasks. Its architecture features a contracting path to capture context and an expansive path for precise localization. The innovative use of skip connections facilitates the flow of fine-grained details across different layers, enhancing the model's ability to accurately delineate object boundaries.

## ERFNet

ERFNet Romera et al. [2018] introduces a novel factorized convolutional layer that significantly reduces the number of parameters while maintaining expressive power. This reduction in parameters enables faster inference without compromising performance, making it well-suited for deployment in resource-constrained environments.

## ResNet

ResNet He et al. [2015] addresses the challenges of training very deep neural networks by employing residual connections. These connections enable the direct flow of information across layers, mitigating the vanishing gradient problem and facilitating the training of extremely deep networks.

## Relevance to our model

We test the performance of the above models on the image segmentation task using the PASCAL VOC-2007 dataset. We look for differences in the models and their relative performance in comparison to the basic fully connected network that we started with.

## Methods

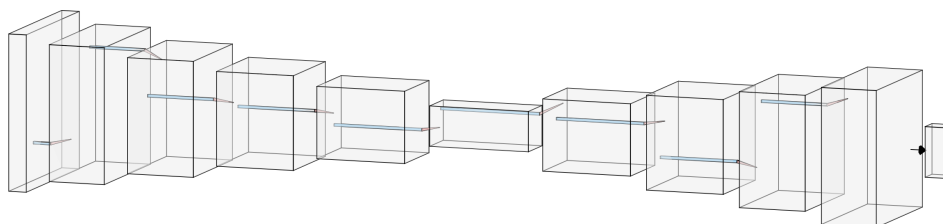


Figure 2: Visualization of System Architecture

## Baseline

Our baseline architecture consists of an encoder, decoder, classifier, and activation. We used the Adam gradient descent optimizer

### Encoder

We have five convolutional layers that increases the depth of the original 3 channels to 32 to 64 to 128 to 256 to 512 each using a size 3 kernel, padding of 1, a stride of 2, and no dilation. Each layer sees a small decrease in the height and width of the layer according to the expression  $\frac{W-F+2P}{2} + 1$ . The outputs of each convolutional layer are subsequently passed through a ReLU activation function and a batch normalization layer.

### Decoder

We have five deconvolutional, or upsampling layers that decreases the depth of the final 512 deep layer output from the encoder. This is decreases from 512 to 256 to 128 to 64 to 32 each using a size 3 kernel, padding of 1, a stride of 2, and no dilation. Each layer sees a small decrease in the height

and width of the layer according to the expression  $S(W - 1) + F - 2P$ . Similarly, the outputs of each deconvolutional layer are subsequently passed through a ReLU activation function and a batch normalization layer.

### **Classifier and Activation**

In our final layer, we have a  $1 \times 1$  convolutional kernel working as a classifier, and a softmax activation layer. This layer projects a probability distribution stream over the 21 classes.

## **Improvements Over Baseline**

### **Data Augmentation**

To enhance the robustness of our model, we applied data augmentation techniques to our dataset. This involved performing various transformations on the input images, such as mirror flips, rotations, and crops. During the process, we must ensure that the same transformations are applied to the corresponding labels to maintain data integrity throughout the augmentation process. We found that data augmentation improved on the average Jaccard index on our models by around 0.03-0.05.

### **Cosine Annealing**

In order to optimize the learning rate dynamically throughout the training process, we implemented the cosine annealing learning rate scheduler. This technique adjusts the learning rate in a cosine-shaped manner, effectively annealing it towards zero as training progresses. By aligning the learning rate adjustments with the number of epochs, we aim to improve the convergence and generalization capabilities of our model. Training our models with cosine annealing had a minimal improvement in both our accuracy and Jaccard index.

### **Class Imbalance**

To mitigate the challenges posed by class imbalance, particularly addressing rare classes, we employed strategies to alleviate this issue. One approach is to apply a weighted loss criterion, which assigns higher weights to the infrequent classes during the optimization process. By doing so, we incentivize the network to pay more attention to these underrepresented classes, thus improving its ability to accurately classify them. Otherwise, the model could simply learn to label the entire image the background and still achieve decent pixel accuracy. The introduction of weight decay had a considerable improvement in our Jaccard index and was used in all our models moving on.

## **Experimentation**

In this work, we introduce DarrenNet, a novel architecture inspired by the erfnet architecture but distinguished by its enhanced efficiency and superior performance. Leveraging a modified erfnet structure, DarrenNet incorporates additional convolution layers and employs higher dropout, resulting in a more intricate and efficient network. The augmented convolutional layers contribute to a deeper understanding of spatial features, while increased dropout aids in regularization, preventing overfitting. The fusion of these modifications yields a model that not only operates more efficiently but also achieves superior performance in various tasks. We are also able to use pretrained erfnet encoders, which improve our performance further.

Below are the descriptions (in table format) and regularization techniques used for each architecture.

## DarrenNet Architecture

Layer	In	Out	Padding	Kernel	Stride	Activation
Initial Block		16	0	3x3	1	ReLU
Downsampler 1	16	64	0	3x3	2	ReLU
Non-bottleneck 1	64	64	0	3x3	1	ReLU
Non-bottleneck 2	64	64	0	3x3	1	ReLU
Non-bottleneck 3	64	64	0	3x3	1	ReLU
Non-bottleneck 4	64	64	0	3x3	1	ReLU
Non-bottleneck 5	64	64	0	3x3	1	ReLU
Downsampler 2	64	128	0	3x3	2	ReLU
Non-bottleneck 6	128	128	0	3x3	1	ReLU
Non-bottleneck 7	128	128	0	3x3	1	ReLU
Non-bottleneck 8	128	128	0	3x3	1	ReLU
Non-bottleneck 9	128	128	0	3x3	1	ReLU
Non-bottleneck 10	128	128	0	3x3	1	ReLU
Non-bottleneck 11	128	128	0	3x3	1	ReLU
Non-bottleneck 12	128	128	0	3x3	1	ReLU
Non-bottleneck 13	128	128	0	3x3	1	ReLU
Upsampler 1	128	64	0	3x3	1	ReLU
Non-bottleneck 14	64	64	0	3x3	1	ReLU
Non-bottleneck 15	64	64	0	3x3	1	ReLU
Upsampler 2	64	16	0	3x3	1	ReLU
Non-bottleneck 16	16	16	0	3x3	1	ReLU
Non-bottleneck 17	16	16	0	3x3	1	ReLU
Output Conv	16	21	0	2x2	2	-

Table 1: DarrenNet Architecture

Layer Name	In	Out	Padding	Kernel Size	Stride	Activation
conv1	$n_{\text{channel}}$	$n_{\text{channel}}$	(1, 0)	3x1	1	ReLU
conv2	$n_{\text{channel}}$	$n_{\text{channel}}$	(0, 1)	1x3	1	ReLU
conv3	$n_{\text{channel}}$	$n_{\text{channel}}$	(1 $\times$ dilated, 0)	3x1	1	ReLU
conv4	$n_{\text{channel}}$	$n_{\text{channel}}$	(0, 1 $\times$ dilated)	1x3	1	ReLU
bn1						
bn2						
dropout						2D

Table 2: Non-bottleneck (DarrenNet)

Layer Name	In	Out	Padding	Kernel Size	Stride	Activation
conv	$in_{\text{channel}}$	$out_{\text{channel}} - in_{\text{channel}}$	1	3x3	2	
pool				2x2	2	
bn	$out_{\text{channel}}$	$out_{\text{channel}}$				

Table 3: DownsamplerBlock (DarrenNet)

Layer Name	In	Out	Padding	Kernel Size	Stride	Activation
conv	$in_{\text{channel}}$	$out_{\text{channel}}$	(1, 1)	3x3	2	
bn	$out_{\text{channel}}$	$out_{\text{channel}}$				

Table 4: UpsamplerBlock (DarrenNet)

## DarrenNet Techniques

In our DarrenNet architecture, we use horizontal and vertical flipping, Kaiming weight initialization, cosine annealing, and add extra penalty to loss inversely proportional to the frequency of a given class pixel.

## Transfer Learning Architecture

Layer	In	Out	Padding	Kernel	Stride	Activation
encoder						
deconv1	512	256	1	3x3	2	ReLU
deconv1	512	256	1	3x3	2	ReLU
deconv2	256	128	1	3x3	2	ReLU
deconv3	128	64	1	3x3	2	ReLU
deconv4	64	32	1	3x3	2	ReLU
conv	32	21	1	3x3	2	Softmax

Table 5: Transferred Encoder to Basic FCN Architecture

## Transfer Learning Techniques

For transfer learning, we used Kaiming weight initialization, cosine annealing, and inverse weight decay. No data augmentation was done on the training set because of the simplicity of the model.

## UNet Architecture

Layer	In	Out	Padding	Kernel	Stride	Activation
conv1	3	64	1	3x3	1	ReLU
conv2	64	64	1	3x3	1	ReLU
pool1	64	64	0	2x2	2	
conv3	64	128	1	3x3	1	ReLU
conv4	128	128	1	3x3	1	ReLU
pool2	128	128	0	2x2	2	
conv5	128	256	1	3x3	1	ReLU
conv6	256	256	1	3x3	1	ReLU
pool3	256	256	0	2x2	2	
conv7	256	512	1	3x3	1	ReLU
conv8	512	512	1	3x3	1	ReLU
pool4	512	512	0	2x2	2	
conv9	512	1024	1	3x3	1	ReLU
conv10	1024	1024	1	3x3	1	ReLU
deconv1	1024	512	0	2x2	2	ReLU
conv11	1024	512	1	3x3	1	ReLU
conv12	512	512	1	3x3	1	ReLU
deconv2	512	256	0	2x2	2	ReLU
conv13	512	256	1	3x3	1	ReLU
conv14	256	256	1	3x3	1	ReLU
deconv3	256	128	0	2x2	2	ReLU
conv15	256	128	1	3x3	1	ReLU
conv16	128	128	1	3x3	1	ReLU
deconv4	128	64	0	2x2	2	ReLU
conv17	64	64	1	3x3	1	ReLU
conv18	64	64	1	3x3	1	ReLU
output	64	21	0	1x1	1	ReLU

Table 6: UNet Architecture

## UNet Techniques

The following techniques were used on UNet: Kaiming weight initialization, frequency weight penalty, cosine annealing, and vertical/horizontal augmentation.

## Results

### Baseline FCN

Our baseline FCN resulted in a 0.06 IOU and a 75% pixel accuracy on the test set.



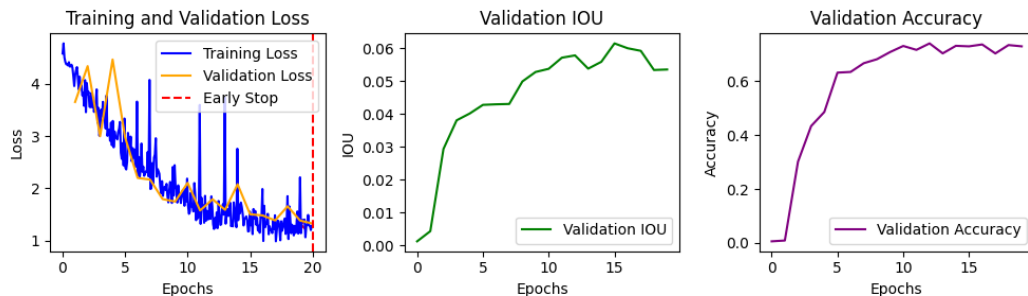


Figure 3: Baseline Augmentation

### FCN with augmentation

Our FCN with augmentation resulted in a 0.06 IOU and a 72% pixel accuracy on the test set. We noticed that the loss convergence was slower.

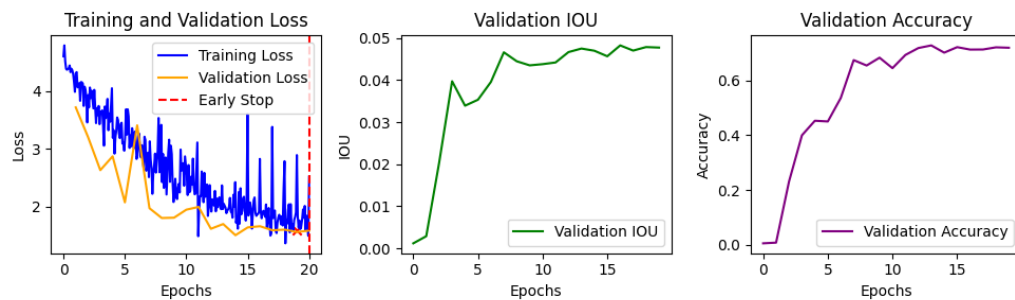


Figure 4: Baseline Augmentation

### FCN with Cosine Annealing LR

Our FCN with Cosine Annealing LR resulted in a 0.05 IOU and a 74% pixel accuracy on the test set.

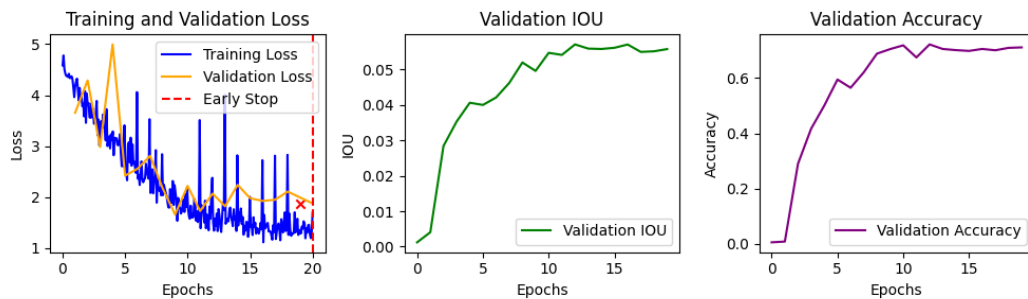


Figure 5: Baseline Cosine

### FCN with Custom Class Weights

Our FCN with custom class weights resulted in a slightly worse 0.04 IOU and a 67% pixel accuracy on the test set.

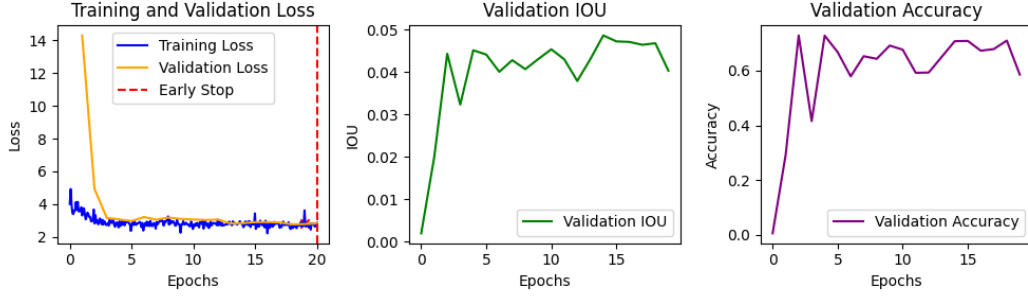


Figure 6: Baseline Weights

### DarrenNet

In Figure 7, we observe the outcomes of DarrenNet. The model has a respectable IOU (0.05) and accuracy (75%), while maintaining very fast training speeds.

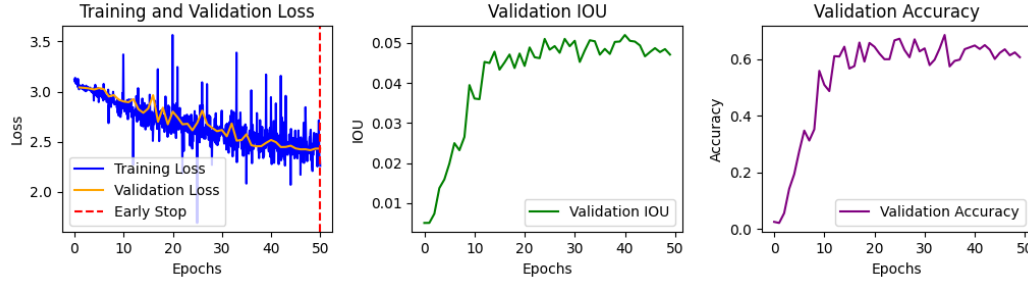


Figure 7: DarrenNet

In Figure 8, we observe the outcomes of DarrenNet with transfer learning using resnet34's encoder. The model leverages pre-trained weights, demonstrating superior performance on the test set. The transfer learning strategy significantly boosts both IOU (0.10) and accuracy (78%), indicating that the network effectively transfers knowledge from the source domain to the target domain.

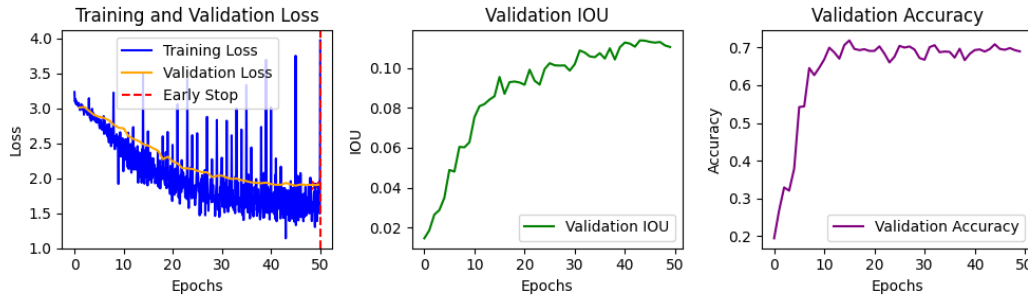


Figure 8: DarrenNet Transfer

Figure 9 represents the results of DarrenNet with both transfer learning and data augmentation. This combination appears to be highly effective, as the model achieves impressive segmentation results on the test set. The incorporation of augmented data during training, along with knowledge transfer, contributes to enhanced generalization capabilities.

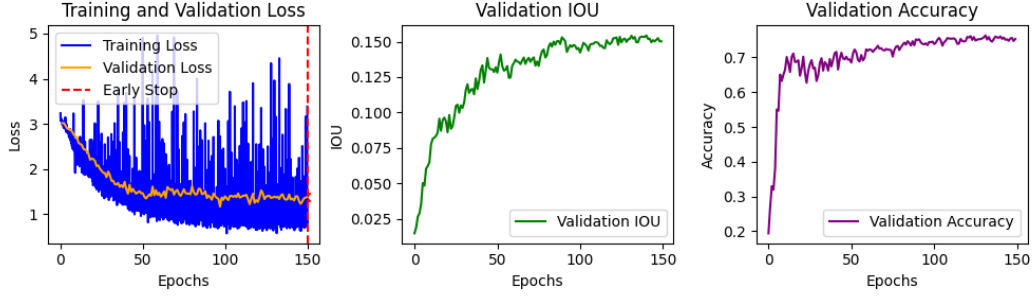


Figure 9: DarrenNet Transfer Augment

Figure 10 displays the results of the DarrenNet with Augment Affine and transfer learning. The model exhibits strong performance on the test set, achieving a high Intersection over Union (IOU) at 0.15 and 82% accuracy. The augmentation techniques, particularly affine transformations, seem to enhance the model's ability to generalize well to unseen data, resulting in improved segmentation accuracy.

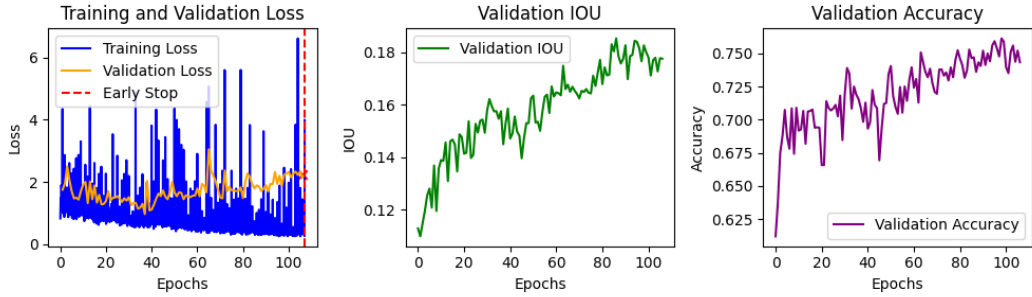


Figure 10: DarrenNet Augment Affine

The UNet architecture's results are depicted in Figure 11. The model demonstrates below average segmentation performance, achieving poor IOU (0.05) and accuracy (0.55) on the test set.

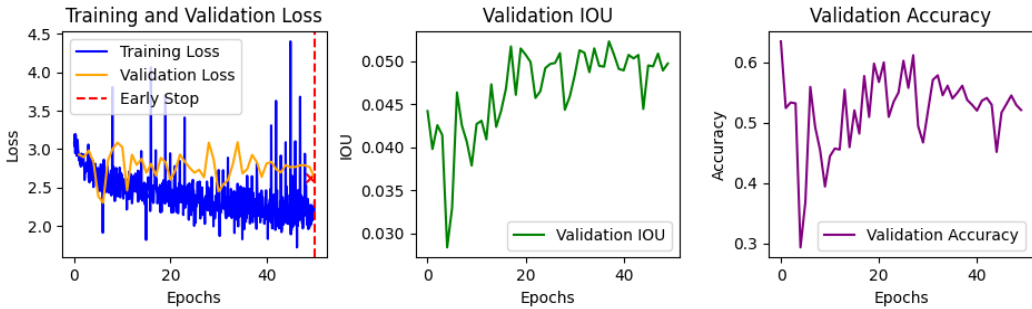


Figure 11: UNet

In Figure 12, we observe the UNet with transfer learning. The model exhibits improved segmentation results compared to the non-transfer counterpart, showcasing the effectiveness of leveraging pre-trained weights. Transfer learning enhances the model's ability to understand and segment structures in the medical images, leading to higher IOU (0.08) and accuracy (79%) on the test set.

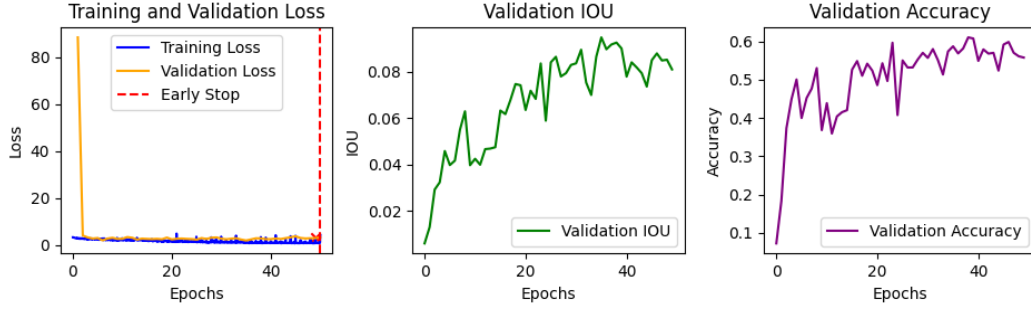


Figure 12: UNet Transfer

We see the best results with DarrenNet that leverages pretrained ERFNet weights. Unet also gives decent results, at least when it comes to detecting humans 13.

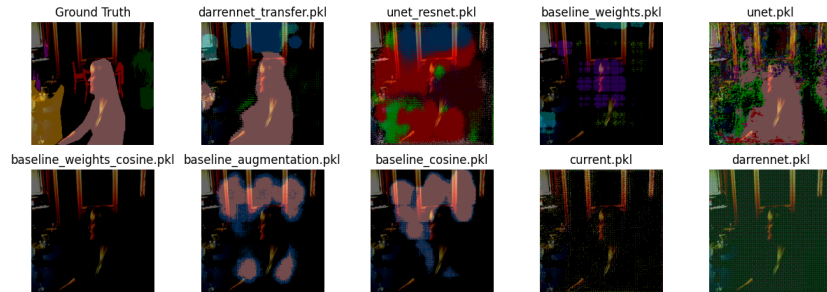


Figure 13: Comparison between models

## Discussion

### Baseline

The baseline model, though straightforward to implement, exhibited limitations in segmentation performance with an IOU of 0.06 and a pixel accuracy of 75%. The simplicity of the architecture hindered its ability to capture intricate features in the data.

### Improved Baseline (FCN with Augmentation)

In an effort to address overfitting, the baseline model was enhanced with data augmentation. Despite these improvements, the model faced challenges with slower loss convergence and only achieved a marginal increase in performance, resulting in an IOU of 0.06 and a decreased pixel accuracy of 72%.

### DarrenNet:

DarrenNet, incorporating advanced architectural features and augmentation techniques such as Affine transformations, displayed notable improvements with an IOU of 0.15 and a pixel accuracy of 82%. The architecture and augmentation strategy played pivotal roles in enhancing segmentation results.

### Transfer Darrennet:

The application of transfer learning with DarrenNet, utilizing pre-trained weights from resnet34, demonstrated significant performance gains with an IOU of 0.10 and a pixel accuracy of 78%. Successful knowledge transfer from the source domain contributed to the improved segmentation performance.

## UNet:

The UNet architecture, characterized by its ability to capture detailed spatial information, showed below-average baseline performance with an IOU of 0.05 and a pixel accuracy of 55%. However, when integrated with transfer learning, UNet outperformed the baseline, achieving an IOU of 0.08 and a pixel accuracy of 79%.

## Performance Differences (Between Implementations):

Comparative analysis revealed that DarrenNet consistently outperformed the baseline, showcasing the significance of architectural enhancements. Transfer learning, as evidenced in both Transfer DarrenNet and UNet with transfer, played a critical role in improving segmentation results, emphasizing the importance of leveraging pre-trained weights for feature extraction.

## Insights from Loss Curves, Tables, Visualizations:

Examination of loss convergence in the improved baseline highlighted challenges in augmentation effectiveness. Visualizations, loss curves, and performance metrics provided insights into the impact of architectural choices and transfer learning strategies, offering valuable information for further model refinement.

## Contributions

**Brandon Szeto:** Basic FCN, model saving and loading, cosine annealing, average IoU and pixel accuracy, architecture research and writeup abstract, introduction, related works, methods.

**Darren Yu:** Group mascot, CUDA support, model inference image preview, plot training versus validation loss, writeup baseline, DarrenNet, and clean/style code.

**Nathaniel Thomas:** Custom CLI, Apple silicon support, dataset augmentation, class imbalance problem, transfer learning using ERFNet, ResNet, and UNet.

## References

Kaiming He, Xiangyu Zhang, Shaoqing Ren, and Jian Sun. Deep residual learning for image recognition, 2015.

Eduardo Romera, José M. Álvarez, Luis M. Bergasa, and Roberto Arroyo. Erfnet: Efficient residual factorized convnet for real-time semantic segmentation, 2018.

Olaf Ronneberger, Philipp Fischer, and Thomas Brox. U-net: Convolutional networks for biomedical image segmentation, 2015.